

This article was downloaded by: [Renmin University of China]

On: 13 October 2013, At: 10:46

Publisher: Taylor & Francis

Informa Ltd Registered in England and Wales Registered Number: 1072954 Registered office: Mortimer House, 37-41 Mortimer Street, London W1T 3JH, UK



Journal of Coordination Chemistry

Publication details, including instructions for authors and subscription information:

<http://www.tandfonline.com/loi/gcoo20>

Syntheses, structures, and fluorescent properties of two new Zn(II) coordination polymers containing 2-((benzoimidazol-yl)methyl)-1H-tetrazole

BINGTAO LIU ^a, DONG ZHAO ^b, TING LI ^b & XIANG-RU MENG ^b

^a School of Environmental and Municipal Engineering, North China Institute of Water Conservancy and Hydroelectric Power, Zhengzhou, 450011, P.R. China

^b The College of Chemistry and Molecular Engineering, Zhengzhou University, Zhengzhou, 450001, P.R. China

Accepted author version posted online: 12 Nov 2012. Published online: 18 Dec 2012.

To cite this article: BINGTAO LIU, DONG ZHAO, TING LI & XIANG-RU MENG (2013) Syntheses, structures, and fluorescent properties of two new Zn(II) coordination polymers containing 2-((benzoimidazol-yl)methyl)-1H-tetrazole, *Journal of Coordination Chemistry*, 66:1, 139-151, DOI: [10.1080/00958972.2012.749351](https://doi.org/10.1080/00958972.2012.749351)

To link to this article: <http://dx.doi.org/10.1080/00958972.2012.749351>

PLEASE SCROLL DOWN FOR ARTICLE

Taylor & Francis makes every effort to ensure the accuracy of all the information (the "Content") contained in the publications on our platform. However, Taylor & Francis, our agents, and our licensors make no representations or warranties whatsoever as to the accuracy, completeness, or suitability for any purpose of the Content. Any opinions and views expressed in this publication are the opinions and views of the authors, and are not the views of or endorsed by Taylor & Francis. The accuracy of the Content should not be relied upon and should be independently verified with primary sources of information. Taylor and Francis shall not be liable for any losses, actions, claims, proceedings, demands, costs, expenses, damages, and other liabilities whatsoever or howsoever caused arising directly or indirectly in connection with, in relation to or arising out of the use of the Content.

This article may be used for research, teaching, and private study purposes. Any substantial or systematic reproduction, redistribution, reselling, loan, sub-licensing,

systematic supply, or distribution in any form to anyone is expressly forbidden. Terms & Conditions of access and use can be found at <http://www.tandfonline.com/page/terms-and-conditions>

Syntheses, structures, and fluorescent properties of two new Zn(II) coordination polymers containing 2-((benzoimidazol-yl)methyl)-1*H*-tetrazole

BINGTAO LIU[†], DONG ZHAO[‡], TING LI[‡] and XIANG-RU MENG^{*‡}

[†]*School of Environmental and Municipal Engineering, North China Institute of Water Conservancy and Hydroelectric Power, Zhengzhou 450011, P.R. China*

[‡]*The College of Chemistry and Molecular Engineering, Zhengzhou University, Zhengzhou, 450001, P.R. China*

(Received 16 April 2012; final version received 27 August 2012)

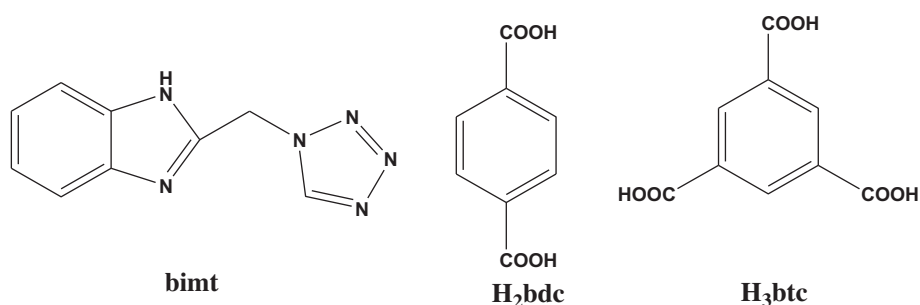
Two coordination polymers, $\{[\text{Zn}(\text{bdc})(\text{bimt})_2]\cdot\text{H}_2\text{O}\}_n$ (**1**) and $\{[\text{Zn}_{1.5}(\text{btc})(\text{bimt})(\text{H}_2\text{O})_3]\cdot\text{H}_2\text{O}\cdot\text{DMF}\}_n$ (**2**), have been synthesized through reactions of 2-((benzoimidazol-yl)methyl)-1*H*-tetrazole (bimt) with $\text{Zn}(\text{NO}_3)_2\cdot 6\text{H}_2\text{O}$ in the presence of 1,4-benzenedicarboxylate (H_2bdc) or 1,3,5-benzenetricarboxylate (H_3btc). Single-crystal X-ray diffraction analyses show that **1** displays a 1-D zigzag chain structure constructed by 1,4-benzenedicarboxylates bridging adjacent Zn(II) ions. Solid **2** shows a 1-D ribbon-like molecular ladder in which three monodentate carboxylates link adjacent Zn1 ions along the crystallographic *a*-direction and connect Zn1 and Zn2 along the crystallographic *c*-axis. In the two polymers, all bimt are terminal ligands to complete the metal coordination sphere and help to assemble the low-dimensional coordination skeleton into high-dimensional ordered supramolecular architectures by N–H···O or N–H···N hydrogen-bonding. IR spectra, fluorescent properties and thermostabilities have been investigated.

Keywords: 2-((Benzoimidazol-yl)methyl)-1*H*-tetrazole; Crystal structure; Fluorescent property; Thermostability

1. Introduction

Coordination polymers have attracted attention not only owing to fascinating topologies, but also to interesting properties and potential applications in ion exchange, luminescence, magnetic, porous materials, gas sorption and storage, molecular recognition and separation, heterogeneous catalysis or catalyst support, drug delivery, and medical imaging [1–12]. Although a large number of complexes have been reported, controlling the exact structures of the final products is a long-term challenge [13]. In the self-assembly processes of metal–organic coordination polymers, many factors influence the formation of final architectures, such as ligands, counterions, temperature, pH, and geometric requirements of the metal ions [14].

*Corresponding author. Email: mxr@zzu.edu.cn



Scheme 1. The ligands involved in this research.

Generally, construction of metal–organic frameworks depends on the nature of the ligands (linkers) and metal ions (nodes) [15]. *N*-heterocyclic compounds have variable coordination modes and adopt a variety of conformations according to restrictions imposed by the coordination geometry of the metal ions [16–18]. For example, flexible multidentate ligands containing imidazole, benzimidazole, triazole, benzotriazole, and tetrazole have been widely employed to construct polymers [19]. Aromatic polycarboxylates have also been widely used as multifunctional ligands, because of various coordination modes to metal ions, from completely or partially deprotonated sites and also the ability to act as H-bond acceptors and donors to assemble supramolecular structures. For instance, benzene dicarboxylate, benzene tricarboxylate, and benzene tetracarboxylate have been used to synthesize polymers. If aromatic polycarboxylate and *N*-heterocyclic organic ligands are introduced into the synthesis at the same time, polymers can be obtained [20–25]. Zn(II) coordinates simultaneously to both oxygen-containing and nitrogen-containing ligands and the final products can exhibit fluorescent properties [26–28]. The aforementioned ideas prompted us to employ 2-((benzoimidazol-yl)methyl)-1*H*-tetrazole (bimt) and 1,4-benzenedicarboxylate acid (H₂bdc) or 1,3,5-benzenetricarboxylate acid (H₃btc) as ligands (Scheme 1) and Zn(II) ion as the centers. In this work, we present two new 1-D Zn(II) coordination polymers, {[Zn(bdc)(bimt)₂]·H₂O}_n (**1**) and {[Zn_{1.5}(btc)(bimt)(H₂O)₃]·H₂O·DMF}_n (**2**), and report fluorescent properties and thermostabilities.

2. Experimental

2.1. General information and materials

The ligand 2-((benzoimidazol-yl)methyl)-1*H*-tetrazole (bimt) was synthesized according to the literature [29]. All chemicals were commercially available and used without purification. IR data were recorded on a NEXUS-470 FTIR spectrometer with KBr pellets from 400–4000 cm⁻¹. Elemental analyses (C, H, and N) were carried out on a FLASH EA 1112 elemental analyzer. The fluorescence spectrum was determined in solid state at room temperature on a Hitachi F-4500 fluorophotometer with excitation and emission slits of 5 nm. PXRD patterns were recorded using Cu-Kα radiation on a PANalytical X'Pert PRO diffractometer. TG measurements were performed by heating the sample from 30 to 700 °C (or 650 °C) at a rate of 10 °C min⁻¹ in air on a NETZSCH STA 409 PC/PG differential thermal analyzer.

2.2. Synthesis of $\{\{Zn(bdc)(bimt)_2\} \cdot H_2O\}_n$ (1)

A mixture of $Zn(NO_3)_2 \cdot 6H_2O$ (0.1 mmol), *bimt* (0.1 mmol), H_2bdc (0.1 mmol), water (5 mL), and DMF (2 mL) was placed in a 25 mL Teflon-lined stainless steel vessel and heated at 353 K for 3 days. After the mixture was cooled to room temperature at a rate of $10^\circ C h^{-1}$, colorless crystals of **1** were obtained (yield: 41% based on Zn). Anal. Calcd for $C_{26}H_{22}N_{12}O_5Zn$ (%): C, 48.20; H, 3.42; N, 25.94. Found: C, 48.25; H, 3.50; N, 25.87. Selected IR (cm^{-1} , KBr): 3384 (m), 3130 (m), 1590 (m), 1560 (s), 1452 (s), 1426 (s), 1393 (m), 1159 (s), 1099 (s), 853 (s), 833 (s), 742 (s), 644 (m).

2.3. Synthesis of $\{\{Zn_{1.5}(btc)(bimt)(H_2O)_3\} \cdot H_2O \cdot DMF\}_n$ (2)

A mixture of $Zn(NO_3)_2 \cdot 6H_2O$ (0.1 mmol), *bimt* (0.1 mmol), H_3btc (0.1 mmol), water (5 mL), and DMF (2 mL) was placed in a 25 mL Teflon-lined stainless steel vessel and heated at 353 K for 3 days. After the mixture was cooled to room temperature at a rate of $10^\circ C h^{-1}$, colorless crystals of **2** were obtained (yield: 56% based on Zn). Anal. Calcd for $C_{21}H_{26}N_7O_{11}Zn_{1.50}$ (%): C, 38.77; H, 4.03; N, 15.07. Found: C, 38.45; H, 3.94; N, 15.11. Selected IR (cm^{-1} , KBr): 3386 (m), 3149 (m), 1698 (s), 1630 (s), 1533 (m), 1452 (m), 1390 (s), 1369 (s), 1170 (m), 1112 (s), 936 (m), 850 (s), 804 (m), 757 (s), 742 (s), 728 (s), 681 (s), 657 (m).

2.4. Single-crystal structure determination

A suitable single crystal of each compound was selected and glued to a thin glass fiber. Crystal structure determinations by X-ray diffraction were performed on a Rigaku Saturn 724 CCD area detector with graphite monochromator for the X-ray source (Mo- $K\alpha$ radiation, $\lambda = 0.71073 \text{ \AA}$) operating at 50 kV and 40 mA. The data were collected in ω scan mode at 293(2) K. The crystal-to-detector distance was 45 mm. An empirical absorption correction was applied and the data were corrected for Lorentz-polarization effects. The structures were solved by direct methods, completed by difference Fourier syntheses and refined by full-matrix least-squares using the SHELXS-97 program package [30]. All non-hydrogen atoms were refined anisotropically. Hydrogens were positioned geometrically and refined using a riding model. The hydrogens were assigned with common isotropic displacement factors and included in the final refinement by using geometrical restraints. Crystallographic parameters and structural refinement for both coordination polymers are summarized in table 1. Selected bond lengths and angles of the two coordination polymers are listed in table 2 and H-bonds in table 3.

3. Results and discussion

3.1. IR spectroscopy of **1** and **2**

The IR spectra of coordination polymers **1** and **2** show absorption bands at 3384 cm^{-1} for **1** and 3386 cm^{-1} for **2** attributed to stretching vibrations of hydroxyl. Absorptions at 3130 cm^{-1} for **1** and 3149 cm^{-1} for **2** originate from Ar-H stretches. Absorptions at 742 cm^{-1} for **1** and 757 and 742 cm^{-1} for **2** correspond to characteristic stretches of

Table 1. Crystal data and structural refinement of **1** and **2**.

Coordination polymers	1	2
Formula	C ₂₆ H ₂₂ N ₁₂ O ₅ Zn	C ₂₁ H ₂₆ N ₇ O ₁₁ Zn _{1.50}
Formula weight	647.93	650.54
Crystal system	Monoclinic	Triclinic
Space group	<i>P2₁/c</i>	<i>P$\bar{1}$</i>
<i>a</i> (Å)	10.669(2)	10.175(2)
<i>b</i> (Å)	16.227(3)	10.743(2)
<i>c</i> (Å)	17.510(6)	12.904(3)
α (°)	90	103.73(3)
β (°)	110.65(3)	96.37(3)
γ (°)	90	98.82(3)
<i>V</i> (Å ³)	2836.7(12)	1337.9(5)
<i>Z</i>	4	2
<i>D_c</i> (g/cm ³)	1.517	1.615
μ /mm ⁻¹	0.926	1.426
Reflns. collected	19,232	14,039
Unique reflns.	5280	4954
<i>R_{int}</i>	0.0477	0.0318
Data / restraints / parameters	5280/0/373	4954/5/367
GOF	1.095	1.055
<i>R₁</i> (<i>I</i> >2 σ (<i>I</i>))	0.0769	0.0484
<i>wR₂</i> (<i>I</i> >2 σ (<i>I</i>))	0.1919	0.1336
<i>R₁</i> (all data)	0.1055	0.0524
<i>wR₂</i> (all data)	0.2115	0.1379

Table 2. Selected bond lengths (Å) and angles (°) for **1** and **2**.

Polymer 1			
Zn(1)–O(4)	1.957(3)	Zn(1)–O(1)	1.981(4)
Zn(1)–N(1)	2.025(4)	Zn(1)–N(7)	2.030(4)
O(4)–Zn(1)–O(1)	124.29(17)	O(4)–Zn(1)–N(1)	102.60(16)
O(1)–Zn(1)–N(1)	105.79(17)	O(4)–Zn(1)–N(7)	107.83(17)
O(1)–Zn(1)–N(7)	105.81(17)	N(1)–Zn(1)–N(7)	110.08(17)
Polymer 2			
Zn(1)–O(7)	1.975(3)	Zn(1)–O(5)#1	1.984(2)
Zn(1)–O(1)	1.987(2)	Zn(1)–N(1)	2.007(3)
Zn(2)–O(3)#2	2.035(3)	Zn(2)–O(3)	2.035(3)
Zn(2)–O(9)#2	2.108(3)	Zn(2)–O(9)	2.108(3)
Zn(2)–O(8)	2.128(3)	Zn(2)–O(8)#2	2.128(3)
O(7)–Zn(1)–O(5)#1	112.02(11)	O(7)–Zn(1)–O(1)	115.13(11)
O(5)#1–Zn(1)–O(1)	98.45(10)	O(7)–Zn(1)–N(1)	115.01(12)
O(5)#1–Zn(1)–N(1)	106.64(11)	O(1)–Zn(1)–N(1)	108.06(12)
O(3)#2–Zn(2)–O(3)	180.000(1)	O(3)#2–Zn(2)–O(9)	88.39(11)
O(3)–Zn(2)–O(9)	91.61(11)	O(9)#2–Zn(2)–O(9)	180.0
O(3)#2–Zn(2)–O(8)	91.19(12)	O(3)–Zn(2)–O(8)	88.81(12)
O(9)#2–Zn(2)–O(8)	87.32(12)	O(9)–Zn(2)–O(8)	92.68(12)
O(8)–Zn(2)–O(8)#2	180.000(1)		

Symmetry transformations used to generate equivalent atoms for **2**: #1: $x+1, y, z$; #2: $-x+2, -y+1, -z+1$.

o-phenylene. Bands at 804, 757, and 681 cm⁻¹ for **2** can be associated with characteristic stretching vibrations of *m*-phenylene. Absorptions at 853 and 833 cm⁻¹ for **1** are from stretches of *t*-phenylene. Separations (Δ) between $\nu_a(\text{COO})$ and $\nu_s(\text{COO})$ are different for unidentate, chelating (bidentate), and bridging coordination polymers. In **1**, unidentate carboxylate exhibits $\nu_a(\text{COO})$ and $\nu_s(\text{COO})$ at 1590 and 1393 cm⁻¹ ($\Delta = 197$ cm⁻¹). In **2**,

Table 3. Hydrogen bonds of **1** and **2**.

D–H···A	<i>d</i> (D–H) (Å)	<i>d</i> (H···A) (Å)	<i>d</i> (D···A) (Å)	(D–H···A) (°)
Polymer 1				
O(5)–H(2 W)···O(2)	0.85	1.95	2.776(8)	163.9
N(2)–H(2B)···O(3)#3	0.86	1.87	2.697(6)	160.6
N(8)–H(8B)···O(5)#4	0.86	1.81	2.663(7)	173.4
O(5)–H(1 W)···N(6)#5	0.85	2.17	3.004(9)	167.7
Polymer 2				
O(9)–H(9B)···O(4)	0.85	1.88	2.695(4)	160.9
O(10)–H(10A)···O(9)	0.84	2.35	3.182(6)	178.0
O(10)–H(10B)···O(1)#2	0.85	2.41	3.257(5)	179.6
N(2)–H(2)···N(6)#4	0.86	2.13	2.974(5)	167.2
O(7)–H(7A)···O(4)#5	0.85	1.92	2.688(3)	150.4
O(7)–H(7B)···O(10)#6	0.85	1.89	2.735(5)	179.4
O(8)–H(8A)···O(11)#7	0.85	2.07	2.883(11)	159.2
O(8)–H(8B)···O(2)#8	0.85	1.86	2.706(4)	170.0
O(9)–H(9A)···O(6)#8	0.85	1.85	2.700(4)	176.9

Symmetry transformations used to generate equivalent atoms for **1**: #3: $x-1, y, z$; #4: $-x+3, -y+3, -z$; #5: $-x+2, -y+2, -z+1$. For **2**: #2: $-x+2, -y+1, -z+1$; #4: $-x+3, -y+3, -z$; #5: $-x+2, -y+2, -z+1$; #6: $x+1, y+1, z$; #7: $-x+2, -y+1, -z$; #8: $x, y-1, z$.

the separation (Δ) between $\nu_a(\text{COO})$ and $\nu_s(\text{COO})$ is 240 cm^{-1} ($1630, 1390 \text{ cm}^{-1}$). Therefore, the carboxylate groups in **1** and **2** coordinate unidentate to zinc [31]. The above analyses were confirmed by X-ray diffraction.

3.2. Crystal structure of $\{[\text{Zn}(\text{bdc})(\text{bimt})_2] \cdot \text{H}_2\text{O}\}_n$ (**1**)

X-ray crystallographic analyses reveal that **1** crystallizes in the monoclinic system with space group $P2_1/c$. The asymmetric unit of **1** contains one Zn(II), one bdc^{2-} , two *bimt*, and one uncoordinated water. As exhibited in figure 1(a), Zn1 is four-coordinate with distorted tetrahedral geometry by two nitrogens (N1, N7) from two monodentate *bimt* ligands and two oxygens (O1, O4) from two monodentate carboxylates. The Zn1–N distances are 2.025(4) and 2.030(4) Å, and the Zn1–O distances are 1.957(3) and 1.981(4) Å, respectively. These bond lengths are close to those in $[\text{Zn}_3(\text{L})(\text{btc})_2(\text{H}_2\text{O})_2] \cdot 3\text{H}_2\text{O}$ (L = 1,2,4,5-tetrakis(imidazol-1-ylmethyl)benzene; $\text{btc} = 1,3,5$ -benzenetricarboxylate) [32].

As depicted in figure 1(b), each bdc^{2-} bridges two Zn(II) ions to form a 1-D zigzag chain ($\cdots\text{Zn}-\text{bdc}^{2-}-\text{Zn}-\text{bdc}^{2-}\cdots$) via Zn1–O coordination. The intrachain Zn···Zn distance separated by bdc^{2-} is 10.980 Å. There are weak $\pi-\pi$ interactions between the benzene and tetrazole rings of adjacent chains. The dihedral angle between these rings is 13.570° and the distance between them is 3.870 Å. As shown in figure 1(c), there are four kinds of intermolecular hydrogen bonds in **1**. N2 of benzimidazole from *bimt* forms a hydrogen bond (N2···O3B: 2.697(6) Å) with O3B of bdc^{2-} ; N8 of benzimidazole from *bimt* forms a hydrogen bond (N8···O5A: 2.663(7) Å) with O5A of uncoordinated water. O5 forms a hydrogen bond (O5···N6A: 3.004(9) Å) with N6A of the tetrazole ring from *bimt*. There are also O–H···O hydrogen bonds (O5···O2: 2.776(8) Å, 163.9°) between uncoordinated water and bdc^{2-} . As illustrated in figure 1(d), existence of these hydrogen-bonds and $\pi-\pi$ interactions further stabilizes the 3-D structure.

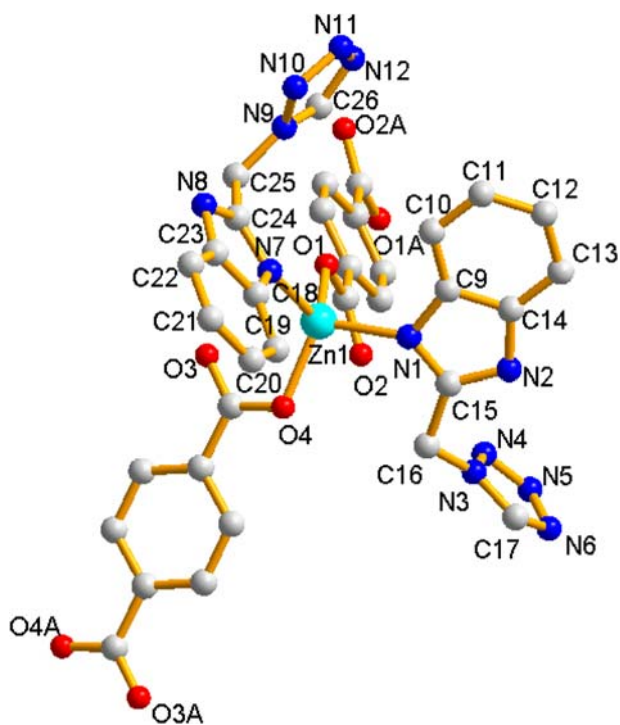


Figure 1. (a) Coordination environment of Zn(II) in **1** with the atom numbering scheme. Hydrogens and uncoordinated water are omitted for clarity.

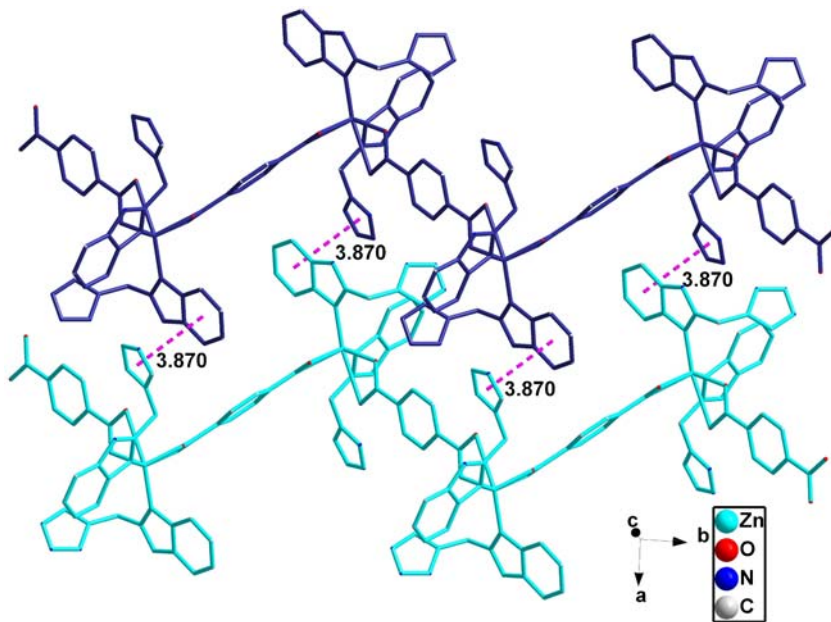


Figure 1. (b) View of the 1-D zigzag chain structure of **1** and π - π interactions between adjacent chains. Hydrogens and uncoordinated water are omitted for clarity.

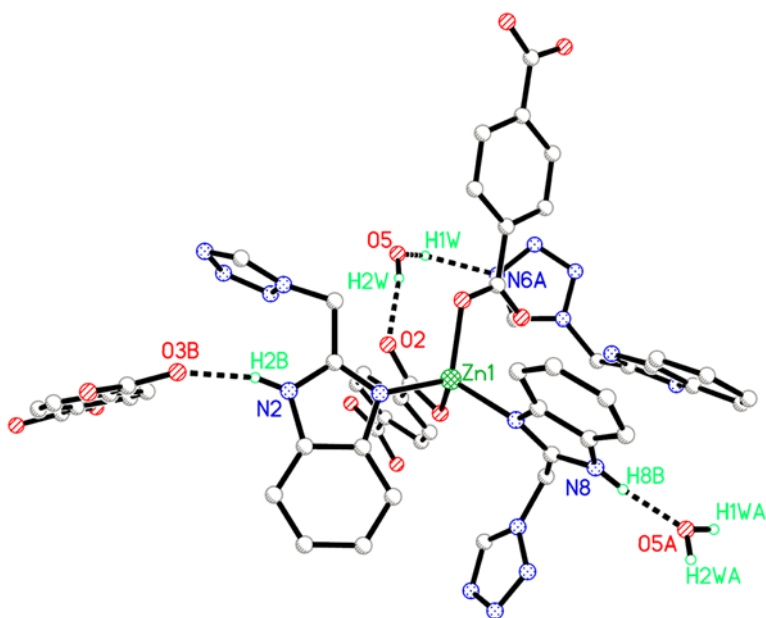


Figure 1. (c) View of hydrogen bonds in **1**.

3.3. Crystal structure of $\{[Zn_{1.5}(btc)(bimt)(H_2O)_3] \cdot H_2O \cdot DMF\}_n$ (**2**)

When H_3btc instead of H_2bdc group was used with other experimental conditions unchanged, **2** with a different structure than **1** is obtained. **2** crystallizes in the triclinic system with space group $P\bar{1}$. The asymmetric unit contains one Zn1, a half of Zn2, one bimt, one btc^{3-} , three coordinated waters, one uncoordinated water, and one uncoordinated DMF. As depicted in figure 2(a), Zn1 is four-coordinate by one nitrogen from monodentate bimt (Zn1–N1=2.007(3) Å), three oxygens from two monodentate carboxylates (Zn1–O1=1.987(2), Zn1–O5B=1.984(2) Å), and one coordinated water (Zn1–O7=1.975(3) Å), exhibiting distorted tetrahedral coordination. The coordination environment of Zn2 is different from Zn1, on an inversion center and six-coordinate by six oxygens from two unidentate carboxylates (Zn2–O3=2.035(3) Å) and four coordinated waters (Zn2–O8=2.128(3), Zn2–O9=2.108(3) Å) in a slightly distorted octahedron. Zn–O and Zn–N bond lengths in **2** are close to those in **1**. O3, O3A, O9, O9A, and Zn2 are located in the same plane. Bond angles around Zn2 are close to 90° or 180°.

As shown in figure 2(b), three carboxylates of btc^{3-} in **2** are monodentate, linking adjacent Zn1 along the crystallographic a -direction and connecting Zn1 and Zn2 along the crystallographic c -axis. As a result, a 1D ribbon-like molecular ladder with terminal bimt as brims is generated. The Zn1–Zn1 distance bridged by btc^{3-} is 10.175 Å. The bimt ligands coordinate monodentate to Zn1 and hang at two sides of the 1-D ribbon-like molecular ladder. As shown in figure 2(c), there are nine kinds of hydrogen-bonding interactions between coordinated water and carboxylate oxygens, between coordinated water and uncoordinated water, between coordinated water and uncoordinated DMF, between the uncoordinated water and carboxylate oxygens, between nitrogen of benzimidazole and nitrogen of tetrazole. As illustrated in figure 2(d), there are π – π interactions between the benzene rings of adjacent chains which are parallel to each other and have an interplanar

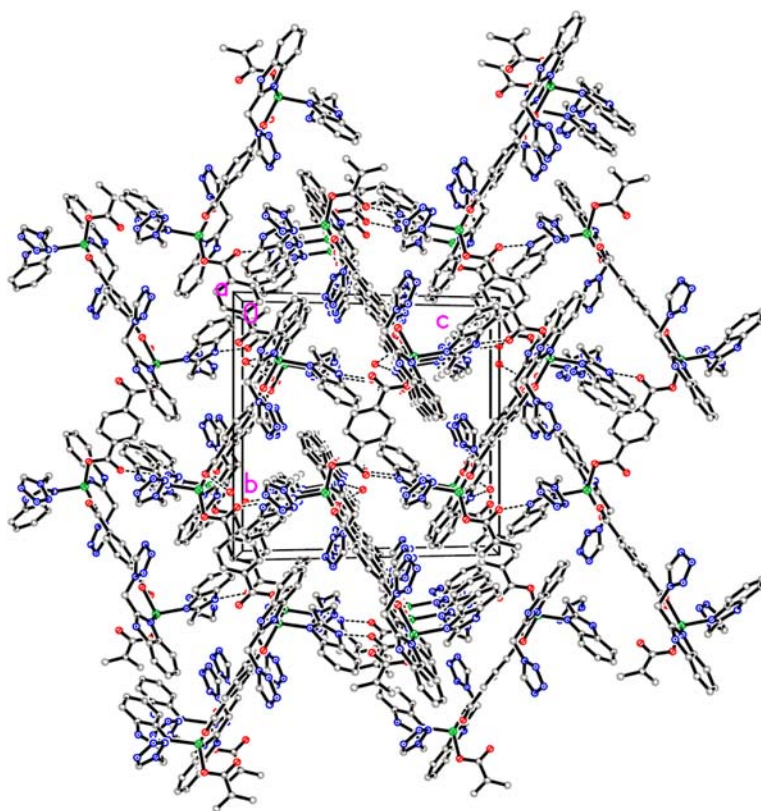


Figure 1. (d) 3-D structure of **1** linked through hydrogen-bonding indicated by dashed lines.

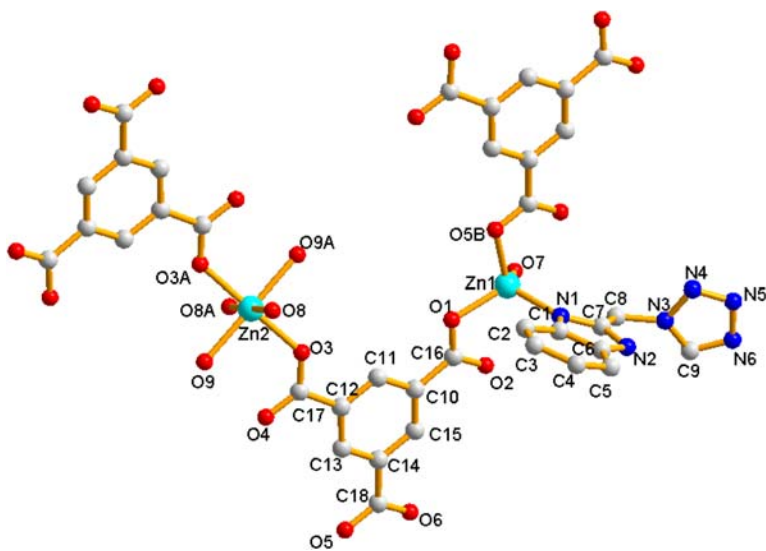


Figure 2. (a) View of coordination sphere around Zn(II) in **2**. Hydrogens, uncoordinated water, and uncoordinated DMF are omitted for clarity.

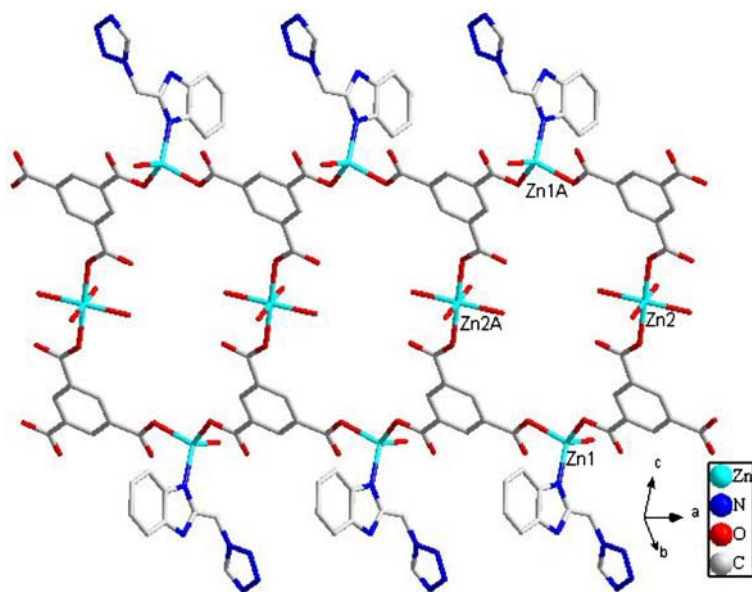


Figure 2. (b) The view of the 1-D chain of **2**. Hydrogens, uncoordinated water, and uncoordinated DMF are omitted for clarity.

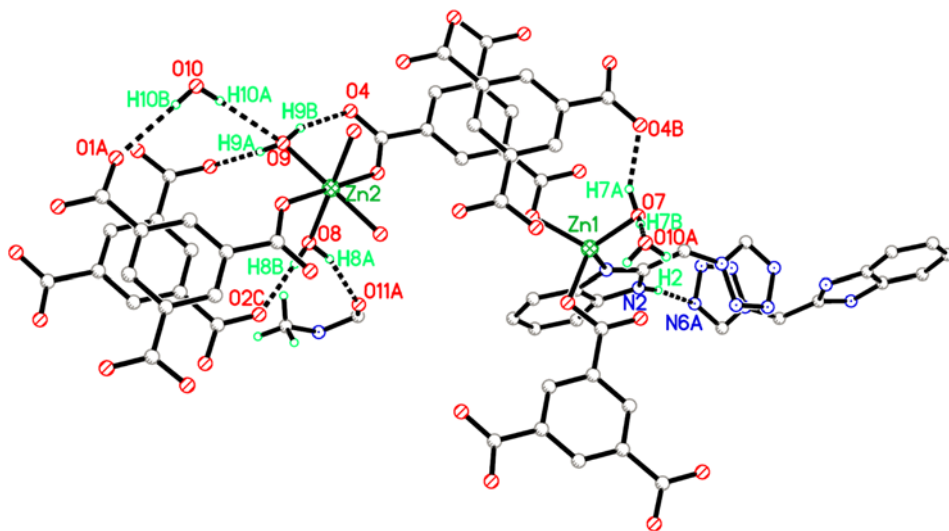


Figure 2. (c) View of hydrogen bonds in **2**.

distance of 3.619 Å. The 1-D chains are further connected by these π - π interactions as well as hydrogen bonds leading to the 3-D structure (figure 2(e)).

As shown in figure SI-1 (Supplementary Material), the computed results show that although there are five potential nitrogen donors in free bimt, the Mulliken atomic charge distributions of nitrogens in the same ligand are significantly different. In bimt, the Mullik-

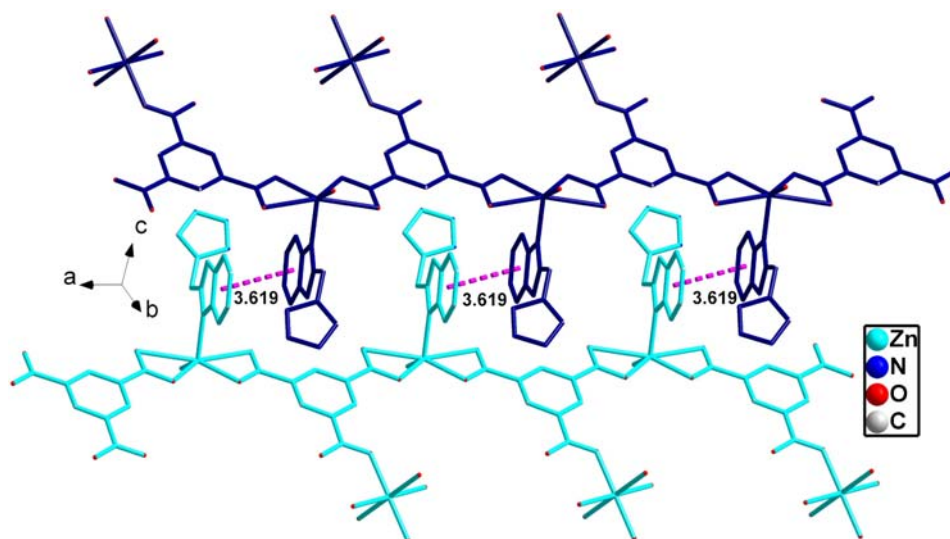


Figure 2. (d) View of the π - π interactions between adjacent chains in **2**.

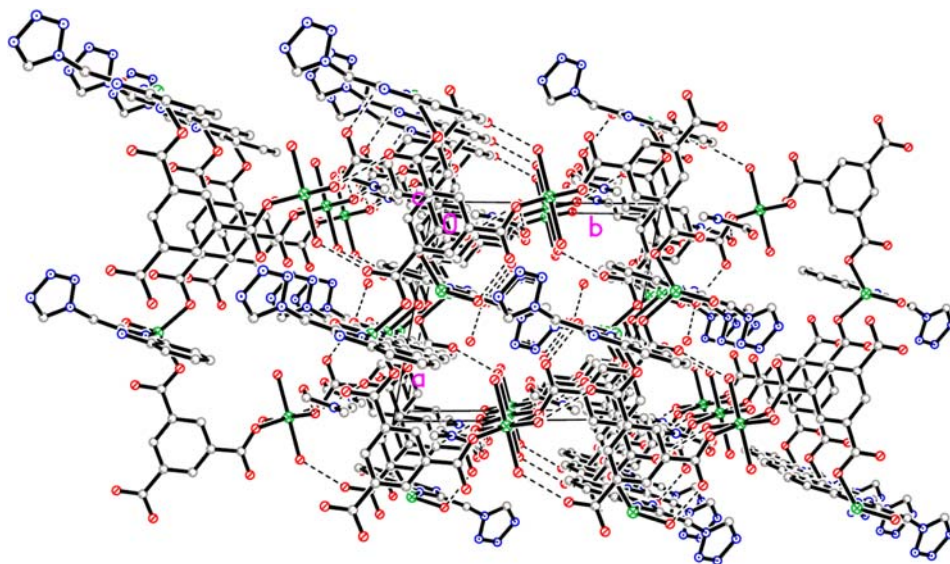


Figure 2. (e) 3-D structure of **2** in the solid state supported by hydrogen bonds.

en charges are -0.263 for N17, -0.358 for N18, -0.160 for N23, but only -0.071 for N21 and -0.074 for N22. So N17, N18, and N23 have comparative advantage in coordinating to metal ions. In addition, considering that protonation of N18 is a great disadvantage for it to coordinate, N17 has an obvious comparative advantage in coordinating to metals. Therefore, bimt can easily coordinate to metal ions as monodentate leading to **1** and **2**. If the reaction conditions are appropriate or N18 can be deprotonated, bimt ligand can be a bridging or tridentate ligand forming 2-D or high-dimensional structures [33].

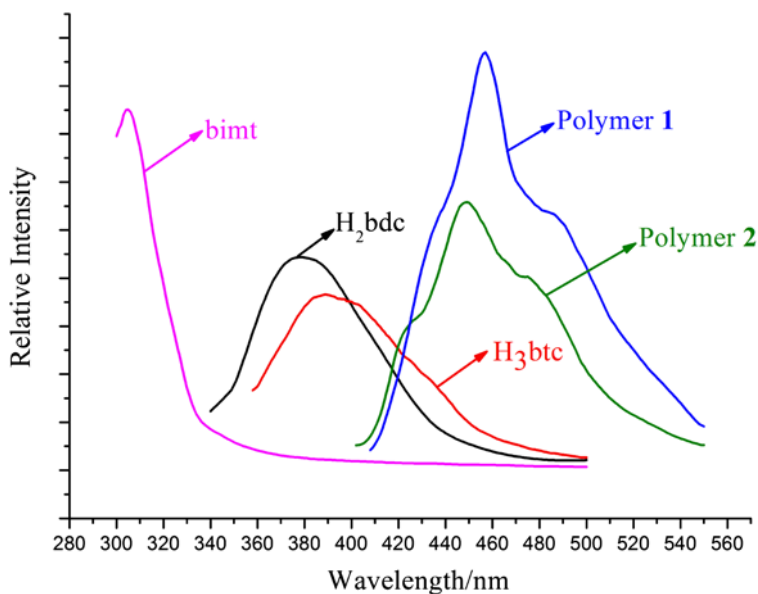


Figure 3. Solid-state photoluminescence spectra of the free bimt, H₂bdc, H₃btc, **1** and **2** at room temperature.

3.4. Fluorescent properties

The excellent fluorescent properties of d¹⁰ metal coordination polymers [34–36] led to investigation of the fluorescence of **1** and **2** in the solid state at room temperature. As shown in figure 3, **1** and **2** display emission bands at 452 nm ($\lambda_{\text{ex}} = 397$ nm) and 448 nm ($\lambda_{\text{ex}} = 392$ nm), respectively. To understand the nature of the emission bands, the fluorescent properties of free bimt, H₂bdc and H₃btc were also measured in the solid state. Free bimt shows an emission band at 302 nm ($\lambda_{\text{ex}} = 283$ nm); H₂bdc and H₃btc molecules give emission bands at 378 nm ($\lambda_{\text{ex}} = 331$ nm) and 389 nm ($\lambda_{\text{ex}} = 347$ nm), respectively. Emissions of **1** and **2** are likely not involved with contributions from bimt. The emission band of **1** may be attributed to intraligand $n \rightarrow \pi^*$ transitions within 1,4-benzenedicarboxylate and the emission band of **2** may be attributed to intraligand $n \rightarrow \pi^*$ transitions within 1,3,5-benzenetricarboxylate ligands [37].

3.5. XRD Patterns

To confirm the phase purity of the two polymers, the PXRD patterns were recorded for **1** and **2**, and they were comparable to the corresponding simulated ones calculated from the single-crystal diffraction data (Supplementary Material, figure SI-2), indicating a pure phase of each bulk sample.

3.6. Thermogravimetric analysis

The TG data of **1** (Supplementary Material, figure SI-3) show that the first weight loss of 2.69% occurred between 56 and 139 °C, corresponding to release of lattice water (Calcd 2.78%). Consecutive weight loss from 187 to 588 °C corresponds to decomposition of 2-

((benzoimidazol-yl)methyl)-1*H*-tetrazole and 1,4-benzenedicarboxylate, respectively. A white granular residue of ZnO (observed 12.71%, calculated 12.60%) remained. The TG curve of **2** (Supplementary Material, figure SI-4) indicates that the first weight loss of 22.03% occurred between 60 and 204 °C, corresponding to the release of lattice and coordination water and *N,N'*-dimethylformamide (calcd. 22.31%). Then there is loss from 211–560 °C, which can be assigned to decomposition of 2-((benzoimidazol-yl)methyl)-1*H*-tetrazole and 1,3,5-benzenetricarboxylate, respectively. The residue of 19.01% should be ZnO (calcd. 18.78%). All these results are in agreement with the crystal structures.

4. Conclusion

The mixed-ligand approach by choice of aromatic polycarboxylic acids and multifunctional *N*-heterocyclic compounds as mixed-linkers is one of the most effective ways to construct coordination polymers [28, 38–41]. Through self-assemblies of a multifunctional *N*-heterocyclic ligand 2-((benzoimidazol-yl)methyl)-1*H*-tetrazole (bimt) with Zn(II) salt in the presence of 1,4-benzenedicarboxylate (H₂bdc) or 1,3,5-benzenetricarboxylate (H₃btc), we obtained two new coordination polymers, {[Zn(bdc)(bimt)₂]·H₂O}_n (**1**) and {[Zn_{1.5}(btc)(bimt)(H₂O)₃]·H₂O·DMF}_n (**2**). Both polymers have 3-D framework structures connected by coordination bonds and hydrogen bonds. Organic counterions can influence the coordination environment of Zn(II), and thus influence the architecture of coordination polymers. Similar behaviors are observed in other coordination polymers based on aromatic polycarboxylic acid ligands and multifunctional *N*-heterocyclic ligands [20, 28, 38–41]. Further efforts on the design and preparation of coordination polymers with other aromatic polycarboxylates and *N*-heterocyclic ligands are underway.

Supplementary material

Crystallographic data for the structures reported in this article in the form of CIF files have been deposited with the Cambridge Crystallographic Data Center as supplementary publication Nos. CCDC 876115 and 876114 for **1** and **2**, respectively. Copies of these data can be obtained free of charge on application to CCDC, 12 Union Road, Cambridge CB2 IEZ, UK (Fax: +44 1223 336 033; E-mail: deposit@ccdc.cam.ac.uk).

Acknowledgment

We gratefully acknowledge the financial support by the National Natural Science Foundation of China (No. J0830412).

References

- [1] L. Brammer. *Chem. Soc. Rev.*, **8**, 476 (2004).
- [2] F. Lloret, G.-D. Munno, M. Julve, J. Cano, R. Ruiz, A. Caneschi. *Angew. Chem. Int. Ed. Engl.*, **37**, 135 (1998).
- [3] N. Lopez, T.-E. Vos, A.-M. Arif, W.-W. Shum, J.-C. Noveron, J.-S. Miller. *Inorg. Chem.*, **45**, 4325 (2006).

- [4] J.-B. Beck, S.-J. Rowan. *J. Am. Chem. Soc.*, **125**, 13922 (2003).
- [5] M.-H. Shu, C.-L. Tu, W.-D. Xu, H.-B. Jin, J. Sun. *Cryst. Growth Des.*, **6**, 1890 (2006).
- [6] S.-S. Chen, M. Chen, S. Takamizawa, P. Wang, G.-C. Lv, W.-Y. Sun. *Chem. Commun.*, **47**, 4902 (2011).
- [7] B. Chen, S. Xiang, G. Qian. *J. Am. Chem. Soc.*, **132**, 1115 (2010).
- [8] H.-L. Jiang, T. Akita, T. Ishida, M. Haruta, Q. Xu. *J. Am. Chem. Soc.*, **133**, 1304 (2011).
- [9] D. Zhao, S. Tan, D. Yuan, W. Lu, Y.-H. Rezenom, H. Jiang, L.-Q. Wang, H.-C. Zhou. *Adv. Mater.*, **23**, 90 (2011).
- [10] B. Liu, H. Shioyama, H. Jiang, X. Zhang, Q. Xu. *Carbon*, **48**, 456 (2010).
- [11] X.-H. Bu, W. Chen, S.-L. Lu, R.-H. Zhang, D.-Z. Liao, W.-M. Bu, M. Shionoya, J. Ribas. *Angew. Chem. Int. Ed.*, **40**, 3201 (2001).
- [12] X.-H. Bu, M.-L. Tong, H.-C. Chang, S. Kitagawa, S.-R. Batten. *Angew. Chem. Int. Ed.*, **43**, 192 (2004).
- [13] J. Kim, B.-L. Chen, T.-M. Reinecke, H.-L. Li, M. Eddaoudi, D.-B. Moler, O.-M. Yaghi. *J. Am. Chem. Soc.*, **123**, 8239 (2001).
- [14] T.-L. Hennigar, D.-C. MacQuarrie, P. Losier, R.-D. Rogers, M.-J. Zaworotko. *Angew. Chem. Int. Ed. Engl.*, **36**, 972 (1997).
- [15] S.-L. Li, Y.-Q. Lan, J.-F. Ma, J. Yang, G.-H. Wei, Z.-M. Cryst. *Growth Des.*, **8**, 675 (2008).
- [16] J. Yang, J.-F. Ma, Y.-Y. Liu, J.-C. Ma, S.-R. Batten. *Cryst. Growth Des.*, **9**, 1894 (2009).
- [17] J.-R. Li, Y. Tao, Q. Yu, X.-H. Bu, H. Sakamoto, S. Kitagawa. *Chem. Eur. J.*, **14**, 2771 (2008).
- [18] J.-R. Li, Y. Tao, Q. Yu, X.-H. Bu. *Chem. Commun.*, **1527**, (2007).
- [19] P.-J. Steel. *Acc. Chem. Res.*, **38**, 243 (2005).
- [20] D. Zhao, Y. Xiu, X.-L. Zhou, X.-R. Meng. *J. Coord. Chem.*, **65**, 112 (2012).
- [21] S.-X. Yan, D. Zhao, T. Li, R. Wang, Y. Xiu, X.-L. Zhou, X.-R. Meng. *J. Coord. Chem.*, **65**, 945 (2012).
- [22] J. Yang, J.-F. Ma, Y.-Y. Liu, J.-C. Ma, S.-R. Batten. *Inorg. Chem.*, **46**, 6542 (2007).
- [23] P.-X. Yin, J. Zhang, Z.-J. Li, Y.-Y. Qin, J.-K. Cheng, L. Zhang, Q.-P. Lin, Y.-G. Yao. *Cryst. Growth Des.*, **9**, 4884 (2009).
- [24] R.-Q. Zou, X.-H. Bu, R.-H. Zhang. *Inorg. Chem.*, **43**, 5382 (2004).
- [25] X.-L. Wang, Y.-F. Bi, G.-C. Liu, H.-Y. Lin, T.-L. Hu, X.-H. Bu. *Cryst. Eng. Comm.*, **10**, 349 (2008).
- [26] N.-W. Ockwig, O. Delgado-Friedrichs, M. O'Keeffe, O.-M. Yaghi. *Acc. Chem. Res.*, **38**, 176 (2005).
- [27] H. Abourahma, B. Moulton, V. Kravtsov, M.-J. Zaworotko. *J. Am. Chem. Soc.*, **124**, 9990 (2002).
- [28] X.-M. Lu, Y.-Y. Chen, P.-Z. Li, Y.-G. Bi, C. Yu, X.-D. Shi, Z.-X. Chi. *J. Coord. Chem.*, **63**, 3923 (2010).
- [29] X.-R. Meng, X.-J. Wu, D.-W. Li, H.-W. Hou, Y.-T. Fan. *Polyhedron*, **29**, 2619 (2010).
- [30] G.-M. Sheldrick. *Acta Cryst.*, **A64**, 112 (2008).
- [31] K. Nakamoto. *Infrared and raman spectra of inorganic and coordination compounds*, Part B, 6th Edn, John Wiley & Sons, Hoboken, NJ (2009).
- [32] Q. Hua, Y. Zhao, G.-C. Xu, M.-S. Chen, Z. Su, W.-Y. Sun. *Cryst. Growth Des.*, **10**, 2553 (2010).
- [33] J. Zhang, B.-D. Li, X.-J. Wu, H.-X. Yang, W. Zhou, H.-W. Hou. *J. Mol. Struct.*, **984**, 276 (2010).
- [34] S.-L. Zheng, J.-H. Yang, X.-L. Yu, X.-M. Chen, W.-T. Wong. *Inorg. Chem.*, **43**, 830 (2004).
- [35] R.-H. Wang, L. Han, F.-L. Jiang, Y.-F. Zhou, D.-Q. Yuan, M.-C. Hong. *Cryst. Growth Des.*, **5**, 129 (2005).
- [36] R. Sun, Y.-Z. Li, J.-F. Bai, Y. Pan. *Cryst. Growth Des.*, **7**, 890 (2007).
- [37] Y.-Y. Liu, J.-F. Ma, J. Yang, Z.-M. Su. *Inorg. Chem.*, **46**, 3027 (2007).
- [38] J.-L. Wang, K.-L. Hou, Y.-H. Xing, Z.-Y. Deng, Z. Shi. *J. Coord. Chem.*, **64**, 3767 (2011).
- [39] K. Akhbari, A. Morsali. *J. Coord. Chem.*, **64**, 3521 (2011).
- [40] L.-N. Yang, Y.-X. Zhi, J.-H. Hei, J. Li, F.-X. Zhang, S.-Y. Gao. *J. Coord. Chem.*, **64**, 2912 (2011).
- [41] P. Zhang, D.-S. Li, J. Zhao, Y.-P. Wu, C. Li, K. Zou, J.-Y. Lu. *J. Coord. Chem.*, **64**, 2329 (2011).